Reactive Extrusion for the Synthesis of Nylon 12 and Maleated Low-Density Polyethylene Blends via the Anionic Ring-Opening Polymerization of Lauryllactam

Libo Du,[1,2] Guisheng Yang[1,3]

[1]*Chinese Academy of Sciences Key Laboratory of Engineering Plastics, Joint Laboratory of Polymer Science and Materials, Institute of Chemistry, Chinese Academy of Sciences, Beijing 100080, People's Republic of China*
[2]*Graduate School of Chinese Academy of Sciences, Beijing 100039, People's Republic of China*
[3]*Shanghai Genius Advanced Materials Company, Limited, Shanghai 201109, People's Republic of China*

Received 3 November 2007; accepted 19 February 2009
DOI 10.1002/app.30293
Published online 8 July 2009 in Wiley InterScience (www.interscience.wiley.com).

ABSTRACT: Nylon 12 was successfully synthesized in a twin-screw extruder via the anionic ring-opening polymerization of lauryllactam (LL). Maleated low-density polyethylene (LDPE–MAH) was added to improve the mechanical properties of nylon 12. The *in situ* blends of nylon 12 and LDPE–MAH were characterized by mechanical testing and scanning electron microscopy. With increasing LDPE–MAH content, the tensile strength and flexural strength decreased, whereas the blend had improved impact strength and achieved supertoughness when the content of LDPE–MAH was 30 wt %. In the *in situ* formed low-density polyethylene-*g*-PA12 copolymer, the domain of the LDPE–MAH phase was finely dispersed in the nylon 12 matrix. The good interface between the two phases demonstrated that LDPE–MAH could be used as a macromolecular activator to induce the polymerization of LL. © 2009 Wiley Periodicals, Inc. J Appl Polym Sci 114: 2662–2672, 2009

Key words: anionic polymerization; nylon; polyethylene (PE); reactive extrusion

INTRODUCTION

The rapid anionic polymerization of lactams has received considerable attention since its discovery in the 1950s.[1–24] Fast reaction kinetics, a clean polymerization reaction without any byproducts, and a crystalline end product make the anionic ring-opening polymerization of lactam a competitive choice for the application of reaction-injection molding, rotational molding, and reactive extrusion and for subsequent continuous shaping to form extrusion profiles and melt-spun fibers. In 1969, Illing[25] wrote the first description of the polymerization of lactams in a corotating twin-screw extruder. He used a ZSK 53 twin-screw extruder to manufacture polyamides 6 and 12 with a molecular weight of 70,000–100,000 g/mol at throughput rates of 27–43 kg/h. The anionic ring-opening polymerization of lactams to generate polyamides has also been studied quite extensively by Sebenda,[9,26] Wichterle and coworkers,[5,10–12] and Gabbert and Hedrick[27] in industry. Caprolactam is by far the most studied lactam, and the nylon 6 prepared by this route compares favorably in properties with that prepared by conventional hydrolytic polymerization. However, the continuous polymerization of lauryllactam (LL) has seldom been studied.[22]

The engineering application of *in situ* polymerized polyamides requires a substantially higher toughness than that given inherently by the related system. This is probably the driving force to develop new systems. According to the additive dissolving properties of lactam, these systems can be divided into two kinds. One is a homogeneous system in which the additive can dissolve in lactam. The other is heterogeneous system in which additive cannot dissolve in lactam. The additives of the former system include polyamide, polystyrene (PS), polyurethane, poly(phenylene oxide), and so on.[28–30] Additives of the latter system include functionalized polypropylene (PP), polyethylene (PE), and so on. Because of the larger interface area between the additives and lactam, it is easier to achieve good dispersion and *in situ* compatibilization for a homogeneous system than for a heterogeneous system. Therefore, it is more difficult to study a heterogeneous system, especially when lactam is the matrix. So far, there have been few reports about

Correspondence to: G. Yang (ygs@geniuscn.com).
Contract grant sponsor: National "973" Program; contract grant number: 2003CB6156002.
Contract grant sponsor: Genius Advanced Material Co., Ltd.

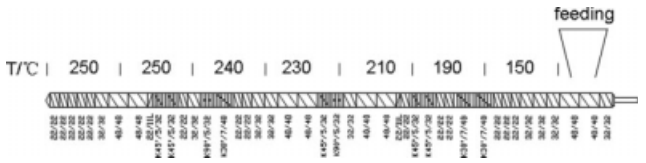

Figure 1 Screw configuration and temperature (T) of zones.

heterogeneous systems. The team of Hu and coworkers[31,32] reported polypropylene (PP) and polyamide (PA6) blends that were synthesized via *in situ* polymerization and *in situ* compatibilization. In their studies, polypropylene-graft-3-isopropenyl-α, α-dimethylbenzene isocyanate (TMI) was used as a macromolecular activator to induce the *in situ* polymerization of caprolactam. The effects of this method on phase dispersion and compatibility were both obvious. However, they only studied the system in which PP was the matrix. What is the situation when lactam is the matrix? Moreover, the mechanical properties of such a system have not been reported.

Compared with PA6, little information is available on toughened nylon 12 (PA12) that has been *in situ* polymerized. Wollny et al.[33] used poly(ethylene-*co*-butyl acrylate) to toughen PA12 by *in situ* formation and compounding. In this system, poly(ethylene-*co*-butyl acrylate) was dissolved in LL. Therefore, it is very challenging to study a heterogeneous reactive system of maleated low-density polyethylene (LDPE–MAH), LL, and other reactants for the synthesis of toughened PA12 blends. In this article, we synthesized toughened PA12 via the polymerization of LL in a twin-screw extruder with LDPE–MAH as an additive. The molecular weights, molecular weight distributions, residual monomer content, blend morphology, and mechanical properties of PA12 and PA12/LDPE–MAH blends were investigated.

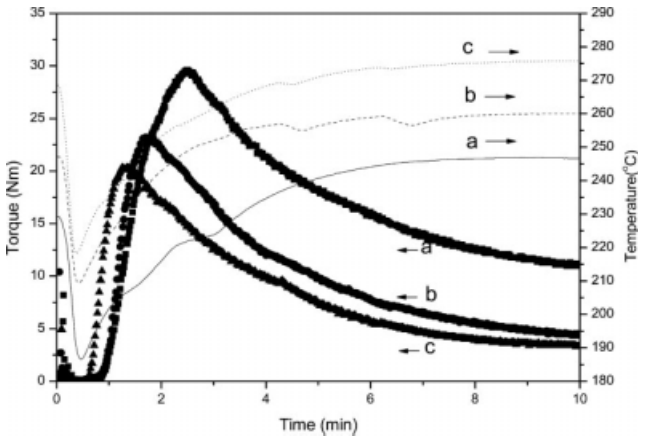

Figure 2 Plots of the torque and material temperature as two functions of time during the polymerization of LL at three different system temperatures: (a) 230, (b) 250, and (c) 270°C. [I]/[A] = 1/1 and [LL]/[A] = 100/1.

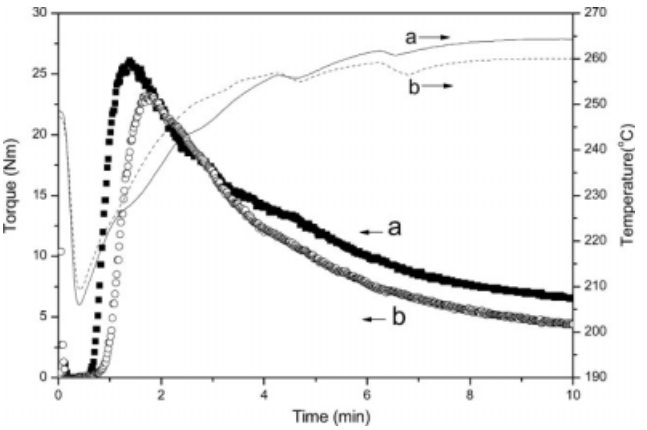

Figure 3 Shows the effect of different initiator/activator ratios ([I]/[A]) on the polymerization at 250°C: (a) [I]/[A] = 2/1 and (b) [I]/[A] = 1/1. [LL]/[A] = 100/1.

EXPERIMENTAL

Materials

LL, with a density of 0.9 g/cm^3, was supplied by Degussa A.G. (Germany), and it was used as received. *N*-Acetyl caprolactam (ACL) as a coinitiator was purchased from Aldrich Chemical Company (Germany). Sodium hydride (NaH) as an initiator was purchased from Shanghai Chemical Reagents Company (China); it contained 45 wt % mineral oil. LDPE–MAH (Surbond ME21G), with a graft ratio of 0.8 wt %, was provided by Lianyong Plastic Technology, Ltd (China).

Processing

Preliminary experiments on anionic LL polymerization with the described initiator/activator system were carried out in a Thermo Haake Polylab system

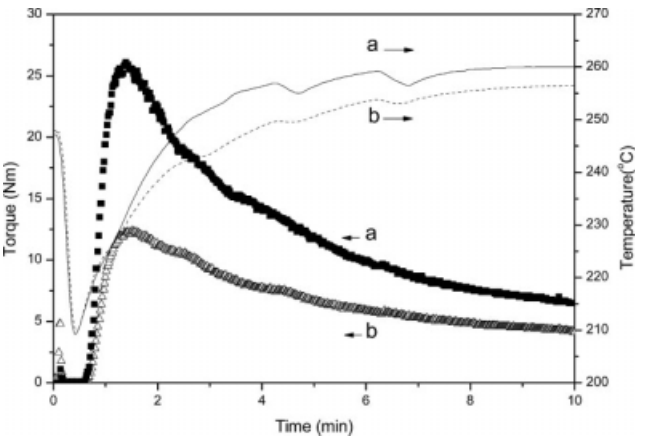

Figure 4 Effect of different monomer/activator molar ratios on the torque and material temperature during the polymerization of LL at 250°C: (a) [LL]/[A] = 100/1 and (b) [LL]/[A] = 50/1. [I]/[A] = 1/1.

TABLE I
Composition of Reactants Used in the Experiment

	LDPE–MAH (g)	LL (g)	NaH (g)	ACL (g)
PA12	0	1000	2.40	8.0
B10	100	900	6.31	7.2
B20	200	800	7.75	6.4
B30	300	700	9.19	5.6
B40	400	600	10.63	4.8

TABLE II
Molecular Weights and Polydispersity Index of Three Different Pure PA12s

[LL]/[A] (mol/mol)	M_n	M_w	Polydispersity index
50/1 (mixer)	11,350	20,089	1.77
100/1 (mixer)	22,453	35,476	1.58
100/1 (TE-35)	21,733	43,273	1.99

The errors of M_n, M_w, and polydispersity index were all less than ±5%.

equipped with a 60-mL mixing chamber. The reaction mixtures were prepared in a 250-mL, round-bottom flask equipped with a magnetic stirrer and a nitrogen inlet. At first, 122 mg (2.54 mmol) of NaH reacted with 50 g (253.8 mmol) molten LL at 170°C; then, the mixture was cooled and made into small solid pellets. ACL (394 mg, 2.54 mmol) was mixed with the pellets with a microinjector. Then, the mixture was added to the chamber. The filling ratio of the internal mixer was between 85 and 90%. The polymerization reactions were performed at three different temperatures: 230, 250, and 270°C. The rotator speed was 60 rpm. After 10 min of reaction time, the melts were quickly quenched between metal plates.

The reactive extrusion polymerization was carried out in an intermeshing corotating twin-screw extruder (TE-35, Nanjing Keya). The length-to-diameter ratio was 38, and the diameter was 35 mm. The configuration of screws, presented in Figure 1, was similar to that of the extruder for the continuous polymerization of ε-caprolactone.[34] The temperatures of different zones are also shown in Figure 1. The first zone was a transporting zone. The second zone was a melting zone where the reactants could be completely molten and achieve preliminary blending. The initiation stage of the reaction occurred in the third zone. Subsequently, the forth zone to the sixth zone were the main reaction zones. The terminal zone was set for volatilization and transporting. Before the polymerization reaction, NaH was reacted with melting LL. Then, the melt mixture was quenched in a dry metal box placed in ice water under purging N_2, which was useful to prevent the initiator from losing activity in open air. The quenched mixture was broken up and premixed with LL, ACL, and LDPE–MAH in a high-speed mixer at a speed of 1000 rpm for 3 min at room temperature. Then, all the materials were fed into zone 0 of a twin-screw extruder at room temperature and protected by a N_2 atmosphere.

The feeding rate was 4 kg/h, and the screw speed was 60 rpm. It was easy to a achieve stable extrusion and a higher conversion of monomer at a low screw speed.[35] The obtained strands were pelletized and dried at 85°C for 24 h. After that, different test specimens for mechanical testing were injection-molded at 260°C. The temperature of the cylinder was 230–250°C, and that of the mold was 40°C. The four blends were denoted as B10, B20, B30, and B40, the number of which is the weight percentage of added LDPE–MAH.

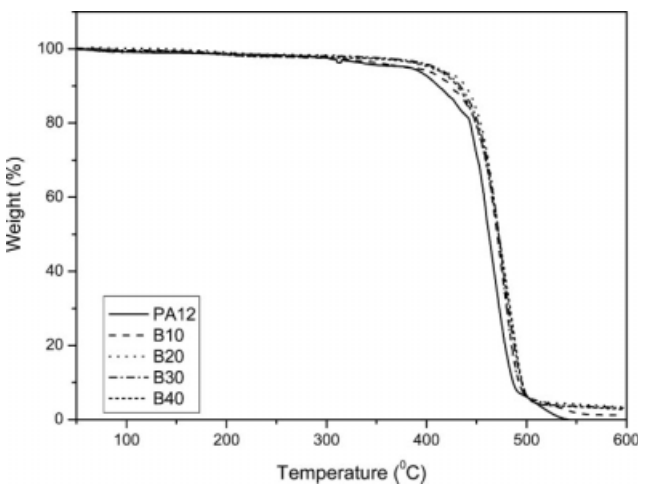

Figure 5 TGA curves of PA12 and PA12/LDPE–MAH blends.

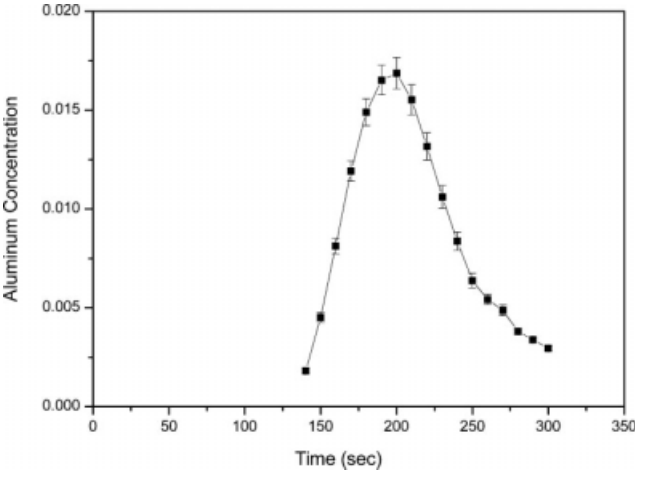

Figure 6 Residence time distribution of PA12 polymerized in a twin-screw extruder with a [LL]/[A] molar ratio of 100/1.

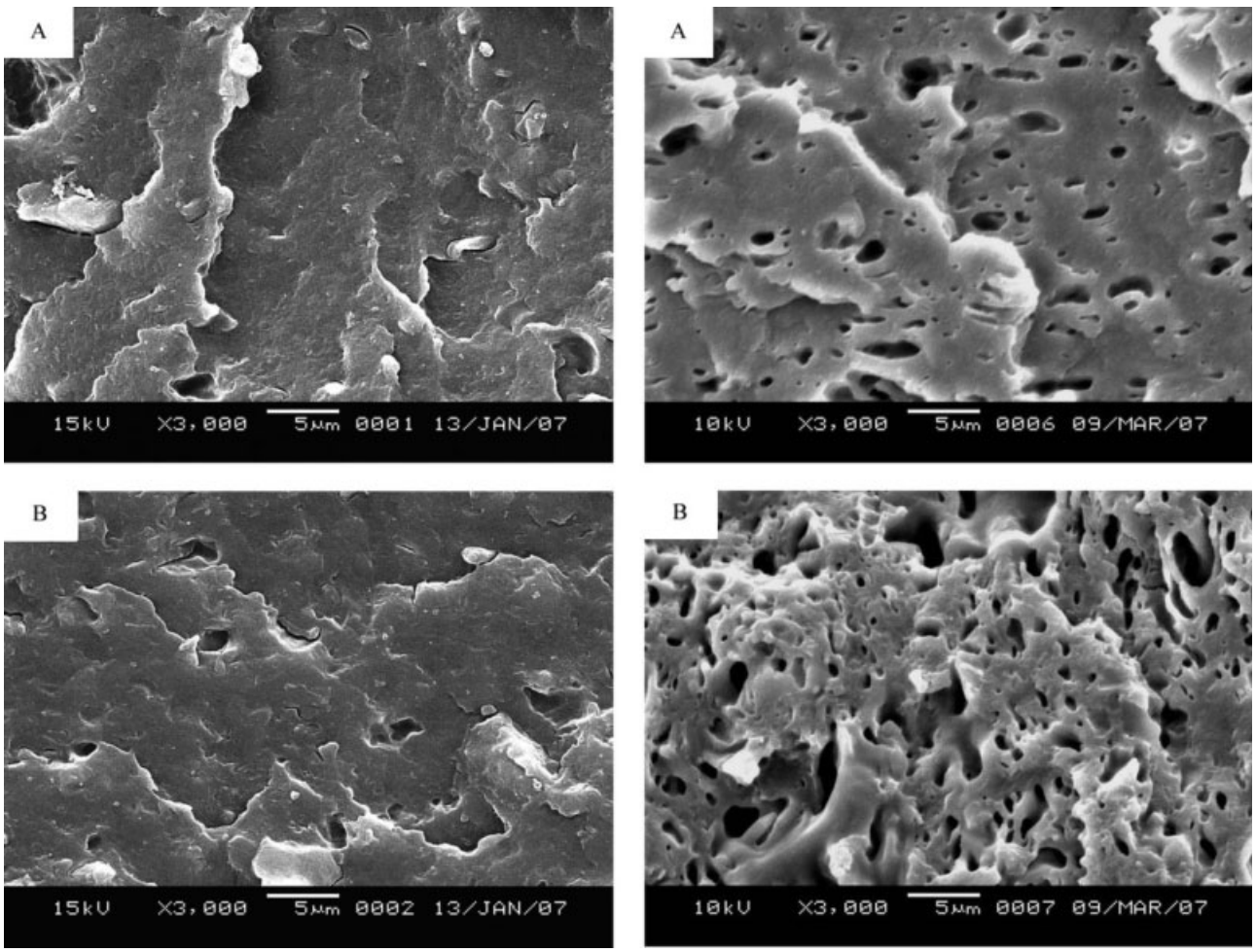

Figure 7 Morphologies of the cryogenic fracture surface (left) and etched surfaces (right) of blends with different LDPE–MAH contents: (A) B10, (B) B20, (C) B30, and (D) B40. The magnification was 3000×.

Determination of the residence time distribution

The residence time distribution for the previous screw configuration was determined with aluminum flakes of a specific weight. The measurements of residence time were carried out during the polymerization of PA12. Aluminum flakes were mixed into the monomer at time zero, and samples were collected every 10 s. The PA12 pellets were burned in an electric muffle furnace at 600°C under air conditions, and the aluminum flakes were separated. The weight of aluminum flakes collected in the extrusion was subsequently measured as a function of time.

Characterization

The residual monomer content in the polyamide was determined by means of thermogravimetric analysis (TGA) with a TA SDT Q600. All TGA measurements were made under a nitrogen atmosphere. The flow rate of N_2 was set at 30 mL/min. The temperature was increased from 30 to 600°C. The scanning rate was 10°C/min, and the initial weights of the samples were 10–15 mg.

The molecular weight of PA12 was measured by gel permeation chromatography (Waters Co., with a refractive-index detector) at 25°C. The solvent was *m*-cresol.

The morphology was observed with a scanning electron microscope (JSM-5610LV, Jeol, Co., Ltd.). The samples were kept in liquid nitrogen for 10 min, and a brittle fracture was performed. Then, the fractured surfaces were etched with xylene at 135°C for 3 h. The etched surfaces of the samples were coated with gold *in vacuo* before observation. The particle size distribution was calculated by our laboratory soft. Both samples were calculated to have at least 200 particles. The number-average diameter (D_n), weight-average diameter (D_w), and volume-average diameter (D_v) were determined as follows:

$$D_n = \frac{\sum N_i D_i}{\sum N_i} \quad (1)$$

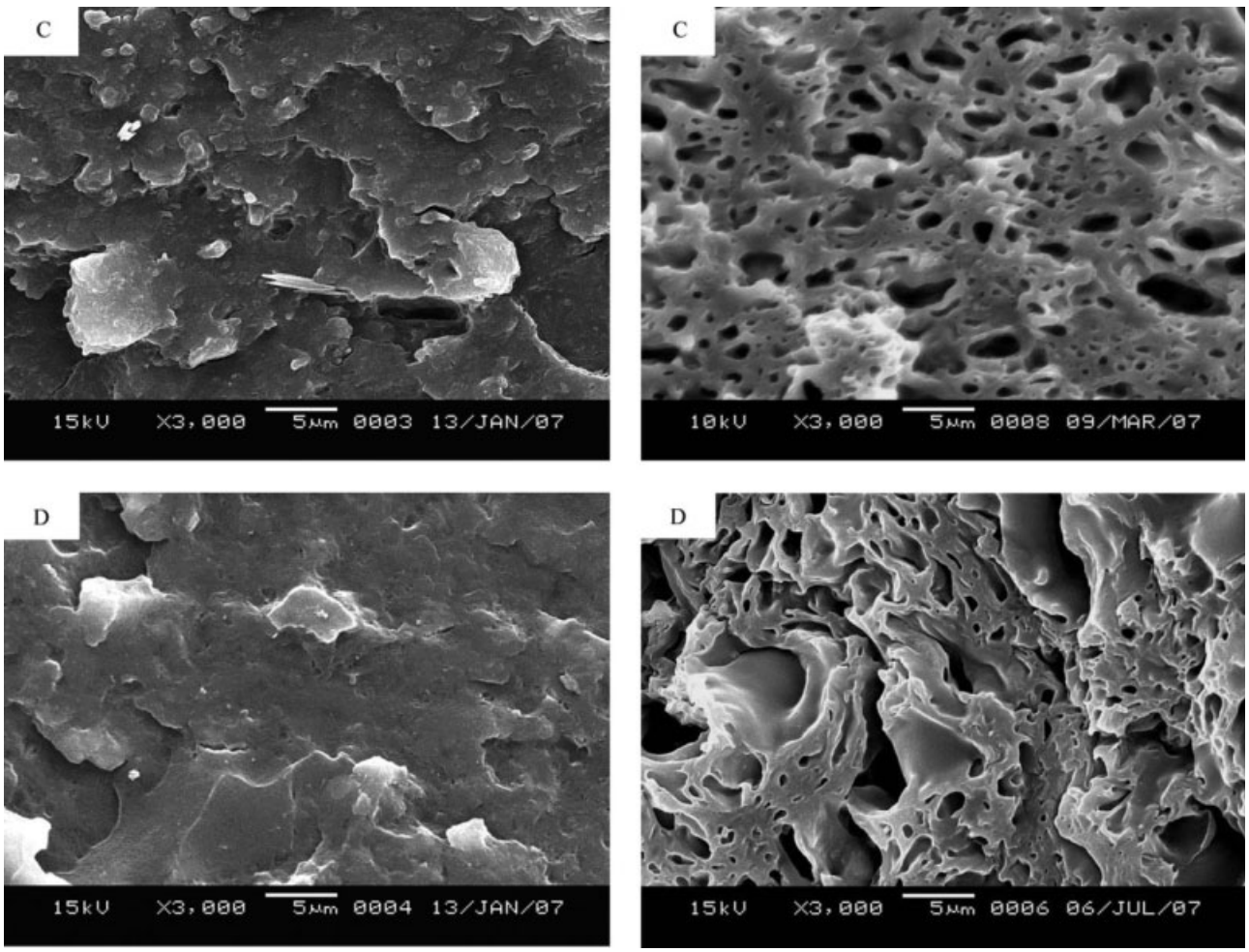

Figure 7 (*Continued from the previous page*)

$$D_w = \frac{\sum N_i D_i^2}{\sum N_i D_i} \quad (2)$$

$$D_v = \frac{\sum N_i D_i^3}{\sum N_i D_i^2} \quad (3)$$

where N_i is the number of domains having diameter D_i.

The tensile properties were evaluated according to ASTM D 638 in an Instron tensile tester (CMT 4204, Shenzhen Xinsansi equipment Co., Ltd.) at a crosshead speed of 50 mm/min. An extensometer strain gauge with a 50-mm gap was used to obtain the modulus and yield stress values. The flexural strength and modulus (ASTM D 790) were tested in the same Instron tensile tester. The dimensions of the flexural specimens were 127 × 12.7 × 3.2 mm^3. The support-to-span ratio was 16. The maximum strain was 5.0%. Notched Izod impact tests were conducted according to ASTM D 256 on an impact testing machine (model XJU-22, Chengde Experiment Equipment Co.). All test specimens were 3.18 mm thick. Six specimens were tested for each mechanical property.

A Rheometrics mechanical spectrometer (ARES rotational rheometer, Rheometrics, Inc.) was used to measure the complex viscosity (η*) and the viscoelastic modulus [dynamic storage modulus (G') and dynamic loss modulus (G'')] as functions of frequency at 200°C. The experiments were carried out in the dynamic mode in parallel-plate geometry at a strain of 5% and a gap of 1.0 mm under dry nitrogen. Sample disks with a diameter of 25 mm were compression-molded with a hot-press machine at a temperature of 200°C. These disks were dried at 80°C *in vacuo* for 48 h before the measurements. The frequency was varied from 0.1 to 100 rad/s, and the amplitude was kept small enough to ensure a linear viscoelastic response of the samples.

RESULTS AND DISCUSSION

Polymerization in an internal mixer

The polymerization of LL was carried out in a Thermo Haake Polylab system first to determine some parameters, such as reactants composition,

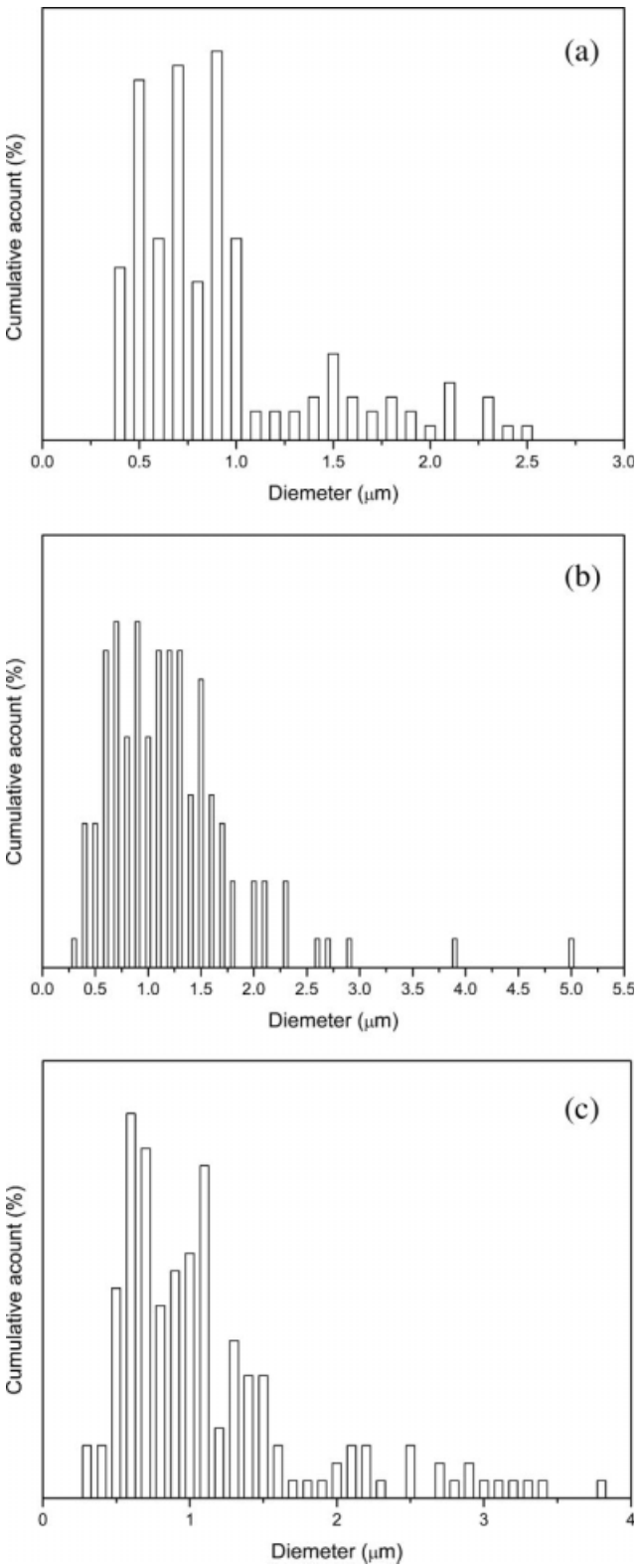

Figure 8 Particle size distributions of blends with different LDPE–MAH contents: (a) B10, (b) B20, and (c) B30.

temperature, residence time, conversion, and torque, of the anionic reaction for subsequent reactive extrusion in the twin-screw extruder. The initiator and activator were NaH and ACL, respectively. The temperature and torque were recorded as functions of time during the polymerization.

Figure 2 shows the torque measurement for the anionic ring-opening polymerization of LL in an internal mixer as a function of time. The slope in the region where the torque increased rapidly corresponded to the reaction rate. As shown in Figure 2, the rate of the anionic ring-opening polymerization became faster at higher temperatures. After it achieved a maximum, the torque decreased with the increasing material temperature. Generally, the torque is related to the viscosity of a material. As shown in Figure 2, the melt viscosity of PA12 was sensitive to temperature and decreased with rising temperature. Also, the terminal temperature in three cases all exceeded the set system temperature. We concluded that there was an effect of self-heating by viscous dissipation in the late stage.

Figure 3 shows the effect of different initiator/activator ratios on the polymerization at 250°C. The different slopes demonstrated that the reaction rate increased as the initiator/activator ratio increased. Figure 4 shows the torque of the synthesized PA12 with different molecular weights by the control of the LL/activator molar ratio ([LL]/[A]) at 250°C. A small ratio led to a low molecular weight of PA12. It was obvious that high-molecular-weight PA12 ([LL]/[A] = 100/1) showed a higher torque and more viscous dissipation than low-molecular-weight PA12 ([LL]/[A] = 50/1) in the whole region.

The conversion of LL was determined by TGA. The loss in weight from 185 to 350°C was attributed to the amount of unreacted LL. The TGA result shows that the residual weights of the PA12 samples with different molecular weights were both higher than 98% at 350°C.

Polymerization in the twin-screw extruder

The reactants feeding into the twin-screw extruder are shown in Table I. The activator amount was proportional to the monomer content, and the content of the initiator increased with increasing LDPE–MAH.

The monomer conversion ratio of PA12 and PA12/LDPE–MAH blends was determined by TGA (Fig. 5). All of the samples exhibited high monomer conversion, above 95 wt %. Moreover, the blends showed a higher volatilizing temperature, about 8°C

TABLE III
Average Diameter of the Three Different Blends

	D_n (μm)	D_w (μm)	D_v (μm)	D_w/D_n
B10	0.88	1.14	1.88	1.30
B20	1.01	1.40	1.75	1.39
B30	1.13	1.70	2.61	1.51

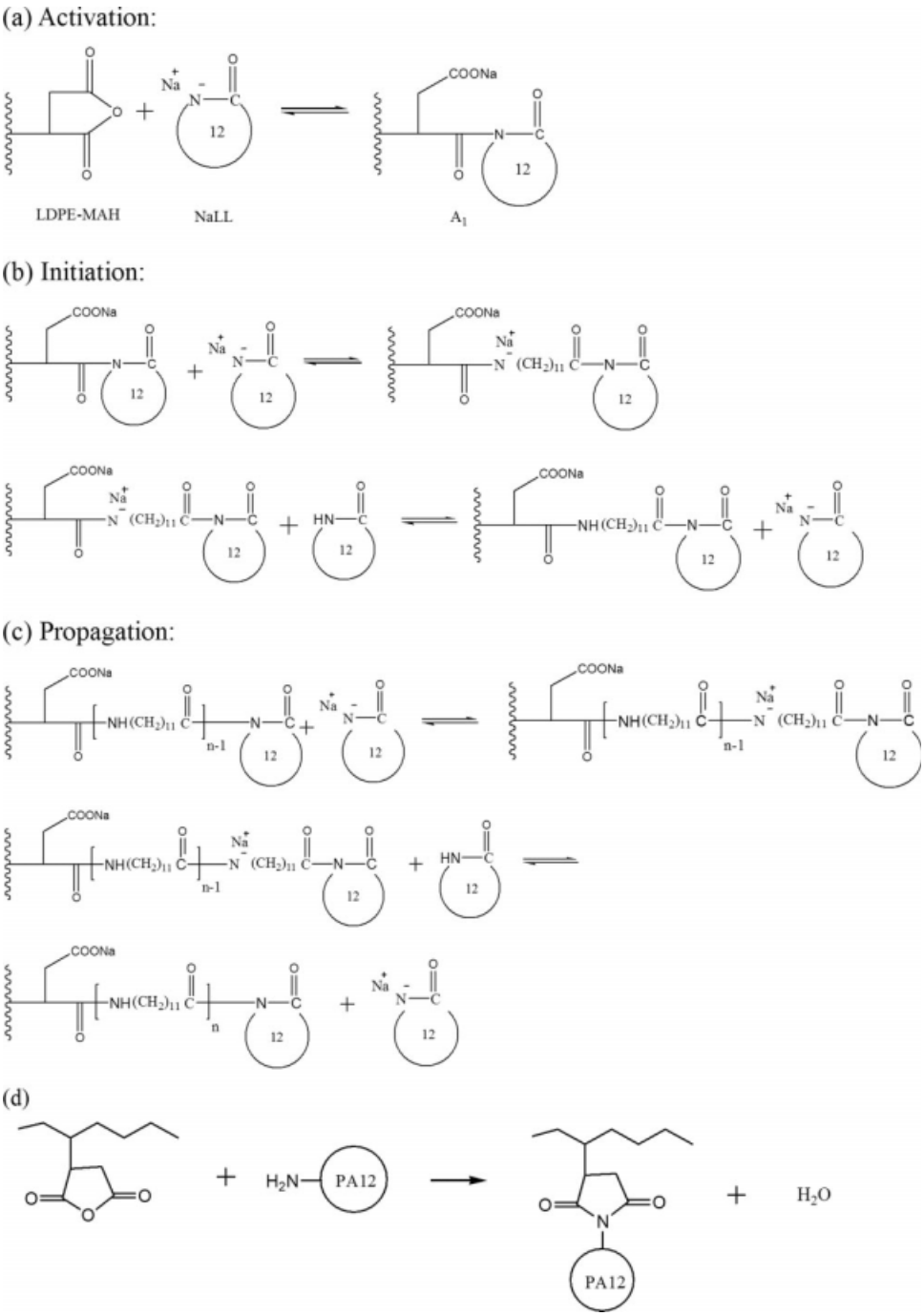

Figure 9 Mechanism of the graft reaction to form LDPE-*g*-PA12.

higher than that of PA12. This remains for further study.

The number-average molecular weight (M_n), weight-average molecular weight (M_w), and polydispersity index of three different pure PA12s are shown in Table II. With the same [LL]/[A] ratio, the polydispersity index of PA12 polymerized in the twin-screw extruder was 1.99, larger than that of PA12 polymerized in the Thermo Haake Polylab system. This was mainly due to the lower residence time and wider residence time distribution (see Fig. 6) in the twin-screw extruder than those in the Thermo Haake Polylab system.

Morphology of the compatibilized blends

Polymer blends, such as the combination of nylon and PE, PP, or PS, have been matters of keen interest because they show high notched Izod impact strength. Nylon/PE, nylon/PP, and nylon/PS blends do not give good dispersion if they are only mechanically blended. However, they show clear

dispersion when they are blended with a maleic anhydride grafted copolymer as a compatibilizer.[36–43] It is very likely that a certain graft polymer is formed between PA and PE, PP, or PS to provide the good dispersion.

The addition of maleated PE can improve the compatibility of components at the interface of a PE/polyamide blend. At the same time, the average dimensions of the dispersed phase decreased, and the interfacial adhesion between PE and PA was also improved. However, the cryogenic fracture was smooth. It was difficult to directly observe the morphology of the dispersed phase on the fracture surfaces of the compatibilized PA12 and PE blends with scanning electron microscopy. Thus, xylene was used to etch the dispersed LDPE–MAH phase. Figure 7 shows the morphologies of PA12 and the LDPE–MAH blends with different weight ratios after cryogenic fracture. The good interfacial adhesion between the two phases was evident because it was difficult to distinguish the two phases. Micrographs of the cryogenic fractured surfaces, which were etched with xylene, are also shown in Figure 7 to describe the dispersion of the LDPE–MAH phase. The irregular edges of the cavities caused by etched LDPE–MAH also demonstrates good interfacial adhesion. The size of the dispersed particles varied from 0.2 to 5 μm. Figure 8 shows the particle size distributions of blends with different LDPE–MAH contents. D_n, D_w, and D_v were calculated and are listed in Table III. With increasing LDPE–MAH, the three kinds of average diameter all increased. D_n was around 1 μm, which was still not the ideal dispersed size for toughening. Founded knowledge is available on this issue because of the success in high-impact polyamides produced by reactive blending. In that case, the rubber modifier was incorporated in the polyamide in a subsequent extrusion process.[44] The impact modifier should be dispersed in the submicrometer range in the polyamide matrix to fulfill its role. The dispersed particles act as stress concentrators and alleviate the triaxial stress state by cavitation, debonding, and matrix-related deformation mechanisms (crazing and shear yielding). Although the dispersed particles of LDPE–MAH were not small enough to achieve the best toughening effect, the high impact strength of the blend with 30 wt % LDPE–MAH indicated that the dispersed domains adhered well to the matrix. Also, with the addition of LDPE–MAH, the index of dispersion (D_w/D_n) only changed a little. This indicated that the distribution of diameter was relatively uniform.

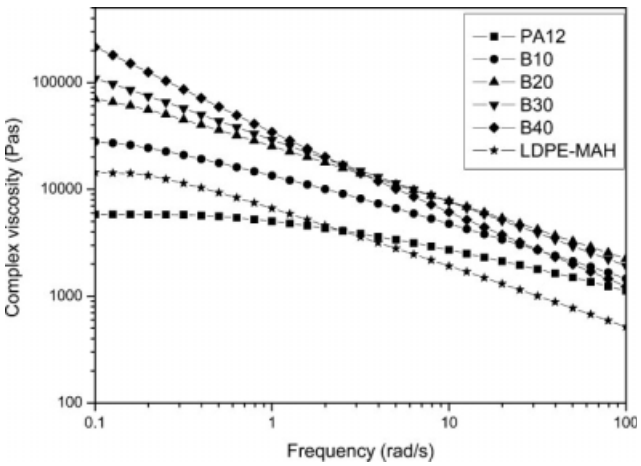

Figure 10 Plots of η* versus frequency for PA12, B10, B20, B30, B40, and LDPE–MAH.

Graft reaction mechanism

During this reactive extrusion, there were mainly two kinds of graft reactions. One was a graft-from mechanism, and the other was a graft-to mechanism. Figure 9(a–c) depicts the graft-from mechanism of the low-density polyethylene (LDPE)-*g*-PA12 graft copolymer formation with LDPE–MAH as the macroactivator. This method was used in our previous work,[45] in which styrene–maleic anhydride copolymer (SMA) was used as the macroactivator in the anionic ring-opening polymerization of caprolactam to synthesize SMA-*g*-PA6 copolymer. There were three main steps involved: activation, initiation, and propagation. Maleic anhydride groups on LDPE–MAH were easy to react with sodium lauryllactam (NaLL) to form acyl LL (A_1; Fig. 9). The acyl LL catalyzed the active anionic polymerization of LL and induced the PA12 chain to grow from these active dots. This graft reaction occurred when the materials were molten and maintained to the end of the anionic ring-opening polymerization in the reactive extrusion. The anionic polymerization of lactams differs from the anionic polymerization of most unsaturated and heterocyclic monomers. The growing center at the chain end is not an anionically activated group but a neutral *N*-acylated lactam, and the anionically activated species is the incoming monomer. The graft-to mechanism is depicted in Figure 9(d). The end amine groups (derived from PA12 chains broken under shearing) on PA12 reacted with the maleic anhydride groups to form imide groups. This is the conventional method to compatibilized polyamide and polyolefin. This kind of graft reaction in extrusion began when a certain amount of PA12 had been polymerized and became more effective when less monomer existed. Compared with the end amine group, a larger amount of NaLL diffused more easily, so NaLL had more of a chance to react with the maleic anhydride groups. Therefore, a graft-from mechanism dominated in the graft reaction.

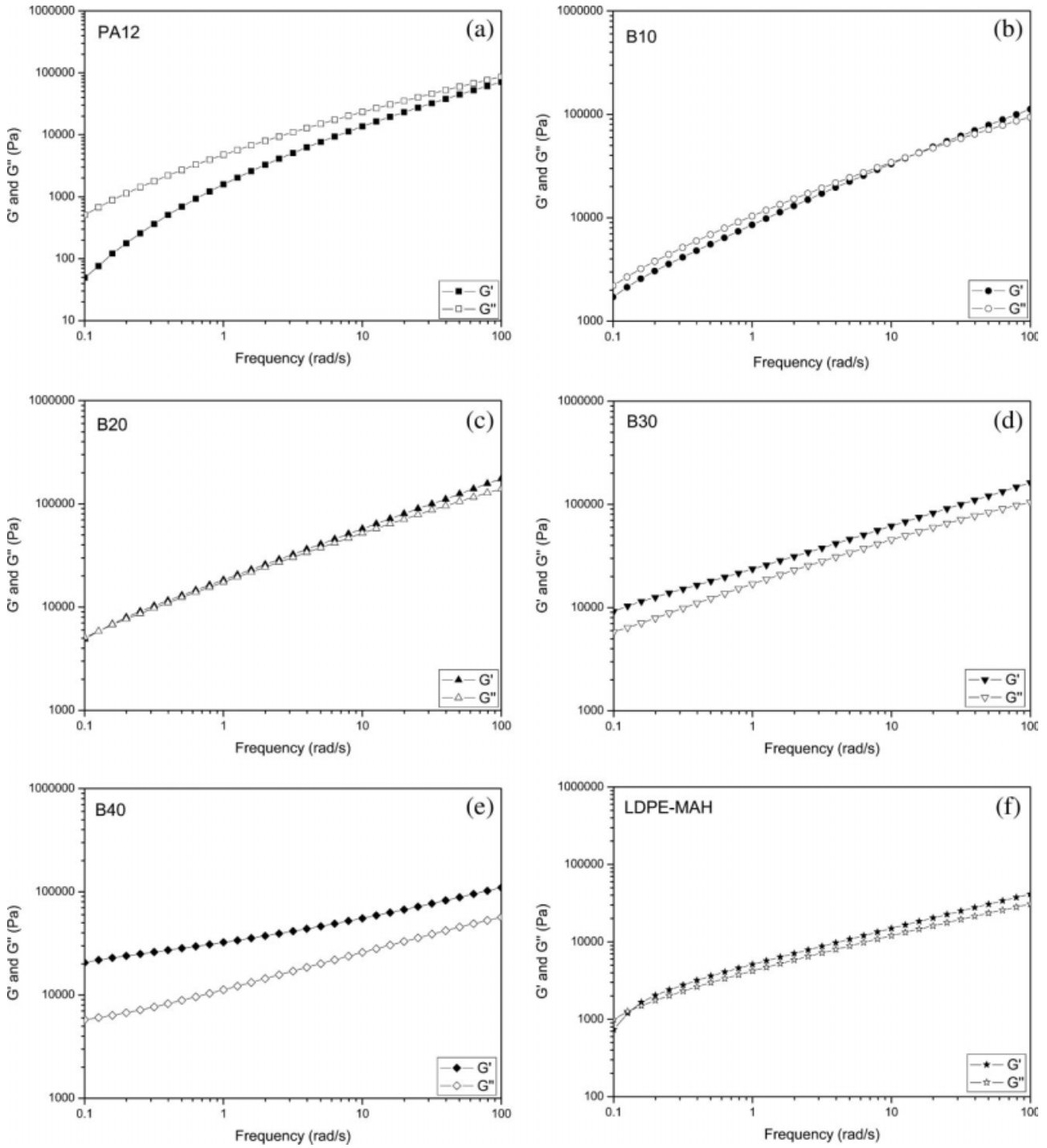

Figure 11 Plots of G' and G'' versus frequency for (a) PA12, (b) B10, (c) B20, (d) B30, (e) B40, and (f) LDPE–MAH.

Dynamic rheological properties

Figure 10 shows plots of η* as a function of frequency for PA12, LDPE–MAH, and their blends. The four blends had higher η* values than PA12 and LDPE–MAH at low frequencies. A progressive increase of η* was observed in the low-frequency range as the content of LDPE–MAH increased. Also, all blends exhibited a typical shear-thinning behavior. Moreover, the shear-thinning behavior became distinct with increasing LDPE–MAH content. This is the typical behavior of a long-branched polymer. The higher viscosity and more distinct shear-thinning behavior proved the existence of LDPE-*g*-PA12, which formed *in situ* via the grafting reaction. There were platforms at low frequency for both PA12 and LDPE–MAH. With increasing LDPE–MAH content, the platforms disappeared gradually. This indicated that the molecular weight distributions of the blends

TABLE IV
Mechanical Properties of PA12, LDPE–MAH, and Their Blends

	Tensile strength (MPa)	Elongation at break (%)	Yield strength (MPa)	Flexural strength (MPa)	Flexural modulus (MPa)	Notched Izod impact strength (J/m)
PA12	53.2 ± 2.4	461 ± 22	46.8 ± 1.1	52.9 ± 2.5	1196 ± 41	88 ± 5
B10	49.2 ± 2.1	506 ± 26	35.7 ± 0.9	34.0 ± 1.2	809 ± 38	135 ± 7
B20	47.2 ± 1.6	479 ± 28	33.0 ± 0.8	33.9 ± 1.5	841 ± 40	536 ± 20
B30	41.8 ± 1.4	407 ± 20	31.1 ± 0.8	29.4 ± 1.4	731 ± 33	947 ± 33
B40	30.7 ± 1.3	314 ± 12		19.4 ± 0.8	446 ± 24	380 ± 18

became wider. In other words, more *in situ* formed LDPE-*g*-PA12 copolymer led to a wider molecular weight distribution.

G' is related to the elastic behavior of a material and may be considered as the storage energy. G'' represents the dissipated energy. The dependence of G' and G'' on the frequency measures the relative motion of all molecules in the bulk and can give important information about the flow behavior of melts. Figure 11 shows plots of G' and G'' as functions of frequency for PA12, LDPE–MAH, and their blends. At low frequency, the two moduli of PA12 decreased more rapidly than those of the blends. The higher the LDPE–MAH content was, the slower the decline of G' and G'' was among the whole frequency range. Also, G' increased faster than G'' from B10 to B40. When the content of LDPE–MAH was above 20 wt %, G' was totally higher than G''. The rheological behavior showed a more elastic trend.

Mechanical properties

The mechanical properties of PA12, LDPE–MAH, and their blends are shown in Table IV. PA12 exhibited excellent tensile properties. The tensile strength of PA12 was 63.2 MPa. The elongation at break of PA12 was 461%, which is high for various polyamide materials. However, the notched Izod impact strength of PA12 was similar to other polyamides, only 88 J/m. Because of the long carbon backbone, the flexural strength and modulus of PA12 were both lower than those of PA6 or Polyamide 66 (PA66). With the addition of LDPE–MAH, the tensile strength of the blend decreased gradually. The degree of the drop was not large from 10 to 30 wt % LDPE–MAH content. The elongation at break increased first and then decreased. This mainly rested with the pristine properties of LDPE–MAH and the adhesion of the two phases. The flexural strength and modulus of the blends decreased with increasing content of LDPE–MAH, so the material became easy to bend. The interesting point of the mechanical properties was the notched Izod impact strength, which increased rapidly and reached a maximum of 947 J/m when the addition of LDPE–MAH was 30 wt % in the blend. Then, the impact strength of the blend with 40 wt % LDPE–MAH addition decreased.

CONCLUSIONS

In this study, we successfully synthesized nylon 12 and LDPE–MAH blends via the anionic ring-opening polymerization of LL in a twin-screw extruder. Because of the *in situ* formed graft copolymer of LDPE-*g*-PA12, the two phases had good adhesion at the interface, and the LDPE–MAH domains were well dispersed in the PA12 matrix. As a result, the notched Izod impact strength of blends improved remarkably. The decreased flexural strength and modulus make the PA12/LDPE–MAH blend more suitable for ductile products. Compared with PA12, the rheological properties of the blends showed higher viscosity and elastic properties, which were ascribed to the large molecular weight of the LDPE-*g*-PA12 copolymer.

References

1. Mottos, E. H.; Hedrick, R. M.; Butler, J. M. U.S. Pat. 3,017,391 (1962).
2. Butler, J. M.; Hedrick, R. M.; Mottos, E. H. U.S. Pat. 3,017,392 (1962).
3. Stehlicek, J.; Sebenda, J.; Wichterle, O. Collect Czech Chem Commun 1964, 29, 1237.
4. Griehl, S.; Schaaf, W. Makromol Chem 1959, 32, 170.
5. Wichterle, O. Makromol Chem 1960, 35, 174.
6. Scella, R. P.; Schonfeld, S. E.; Donaruma, L. G. J Appl Polym Sci 1964, 8, 1363.
7. Stechlicek, J.; Labsky, J.; Sebenda, J. Collect Czech Chem Commun 1967, 32, 370.
8. Sittler, E.; Sebenda, J. Collect Czech Chem Commun 1968, 33, 270.
9. Sebenda, J. J Macromol Sci Chem 1972, 6, 1145.
10. Wichterle, O.; Sebenda, J.; Kralicek, J. Br. Pat. 904,229 (1962).
11. Wichterle, O.; Sebenda, J.; Kralicek, J. U.S. Pat. 3,200,095 (1965).
12. Wichterle, O.; Sebenda, J.; Kralicek, J. U.S. Pat. 3,166,533 (1965).
13. Steinhofer, A.; Dachs, K.; Brueggemann, H.; Shurtz, E.; Willhelm, H. Br. Pat. 919,246 (1962).
14. ICI Br. Pat. 944,307 (1963).
15. Illing, G.; Zahradnik, F. U.S. Pat. 3,371,055 (1968).
16. Reinking, K.; Vogel, H.; Hechelhammer, W.; Schneider, K. U.S. Pat. 3,676,544 (1972).

17. Ivanova, S. L.; Kadrashev, V. V.; Korchagina, M. A. Int Polym Sci Technol 1974, 1, T76.
18. Biensan, M.; Potin, P. U.S. Pat. 4,067,861 (1978).
19. Alijev, R.; Budesinky, M.; Kondel, J.; Kova, K. J Angew Makromol Chem 1982, 105, 107.
20. Bartilla, T.; Kirch, D.; Nordmeier, J.; Promper, E.; Strauch, T. Adv Polym Technol 1986, 6, 339.
21. Menges, G.; Bartilla, T. Polym Eng Sci 1987, 27, 1216.
22. Ha, S. K.; White, J. L. Int Polym Process XIII 1998, 2, 136.
23. Kye, H.; White, J. L. J Appl Polym Sci 1994, 52, 1249.
24. Kye, H.; White, J. L. Int Polym Process 1966, 11, 129.
25. Illing, G. Mod Plast 1969, 46(8), 70.
26. Sebenda, J. Prog Polym Sci 1978, 6, 123.
27. Gabbert, J. D.; Hedrick, R. M. Polym Process Eng 1986, 4, 359.
28. Li, Y. L.; Yang, G. S. Macromol Rapid Commun 2004, 25, 1714.
29. Hou, L. L.; Yang, G. S. Polym Int 2006, 55, 643.
30. Hou, L. L.; Yang, G. S. Polym Eng Sci 2006, 46, 1196.
31. Hu, G. H.; Cartier, H.; Plummer, C. Macromolecules 1999, 32, 4713.
32. Hu, G. H.; Huxi, L.; Feng, L. Polymer 2005, 46, 4562.
33. Wollny, A.; Nitz, H.; Faulhammer, H.; Hoogen, N.; Mülhaupt, R. J Appl Polym Sci 2003, 90, 344.
34. Machado, A. V.; Bounor-Legare, V.; Goncalves, N. D.; Melis, F.; Cassagnau, P.; Michel, A. J Appl Polym Sci 2008, 110, 3480.
35. Kim, I.; White, J. L. J Appl Polym Sci 2005, 97, 1605.
36. Ide, F.; Hasegawa, A. J Appl Polym Sci 1974, 18, 963.
37. Chen, C. C.; Fontan, E.; Min, K.; White, J. L. Polym Eng Sci 1988, 28, 69.
38. Hobbs, S. Y.; Bopp, R. C.; Watkins, V. H. Polym Eng Sci 1983, 23, 380.
39. Utracky, L. A.; Dumoulin, M. M.; Toma, P. Polym Eng Sci 1986, 26, 34.
40. Heikens, D.; Barensten, W. Polymer 1977, 18, 69.
41. Heikens, D.; Hoen, N.; Barensten, W.; Piet, P.; Ladan, H. J Polym Sci Polym Symp 1978, 62, 309.
42. Barensten, W. M.; Heikens, D.; Piet, P. Polymer 1974, 15, 119.
43. Mascia, L.; Xanthos, M. Adv Polym Tech 1992, 11, 23.
44. Keskkula, H.; Paul, D. R. In Nylon Plastics Handbook; Kohan, M. I., Ed.; Hanser: Munich, 1995.
45. Du, L. B.; Yang, G. S. J Appl Polym Sci 2008, 108, 3419.